

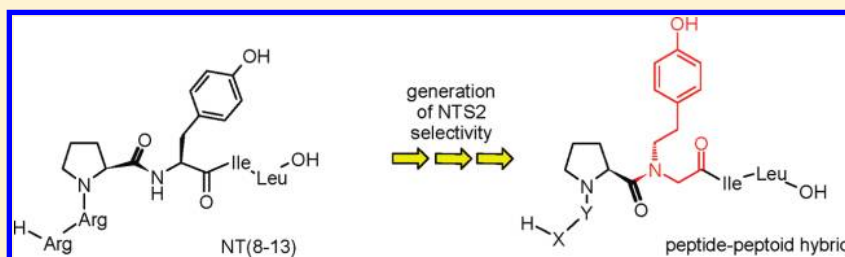
## Discovery of Highly Potent and Neurotensin Receptor 2 Selective Neurotensin Mimetics

Jürgen Einsiedel, Cornelia Held, Maud Hervet, Manuel Plomer, Nuska Tschammer, Harald Hübner, and Peter Gmeiner\*

Department of Chemistry and Pharmacy, Emil Fischer Center, Friedrich Alexander University, Schuhstrasse 19, 91052 Erlangen, Germany

**S** Supporting Information

### ABSTRACT:



The neurotensin receptor subtype 2 (NTS2) is involved in the modulation of tonic pain sensitivity and psychiatric diseases and is, therefore, regarded as a highly attractive pharmacological target protein. Aiming to discover NTS2 selective ligands, we herein describe the identification of screening hits and the chemical synthesis of structural variants leading to the highly potent and NTS2 selective peptide-peptoid hybrids of type 3. The neurotensin mimetics **3a** and **3e-g** incorporating an *N*-(4-hydroxyphenethyl)-glycine substructure exhibit single digit nanomolar affinity ( $K_i = 4.3\text{--}8.8\text{ nM}$ ) and 1900–12000 fold selectivity over the neurotensin receptor subtype 1 (NTS1). According to functional experiments, the test compounds **3a** and **3e-g** displayed an inhibition of constitutive mitogen-activated protein kinase (MAPK) activity exceeding 2.6–4.6 times the inverse agonist activity of the endogenous ligand neurotensin.

### INTRODUCTION

The tridecapeptide neurotensin (pGlu-Leu-Tyr-Glu-Asn-Lys-Pro-Arg-Arg-Pro-Tyr-Ile-Leu-OH) is widely distributed in the brain and in the gastrointestinal tract.<sup>1,2</sup> Neurotensin exerts a variety of physiological effects including hypothermia,<sup>3</sup> analgesia,<sup>4</sup> and antipsychotic properties.<sup>5</sup> The C-terminal hexapeptide NT(8–13) with the sequence H-Arg-Arg-Pro-Tyr-Ile-Leu-OH (**2**, Figure 1) proved to be the pharmacologically active motif<sup>6</sup> and has become the lead structure for the development of neurotensin derived drugs and imaging agents (Figure 1).<sup>7,8</sup> The biological effects are mediated by two G-protein coupled receptor (GPCR) subtypes including the high affinity, levocabastine-insensitive receptor NTS1,<sup>9,10</sup> and the low affinity, levocabastine-sensitive subtype NTS2.<sup>11,12</sup> The neurotensin receptor subtype 3 (NTS3) belongs to the Vps10p family of sorting receptors, which contain a single transmembrane domain.<sup>13</sup>

The focus of neurotensin receptor research was mainly directed to NTS1, which is expressed in the central nervous system (CNS) and in peripheral organs.<sup>10</sup> NTS1 appears to be associated with the analgesic and antipsychotic effects of neurotensin and was, therefore, evaluated as a drug target. As a negative prognostic marker,<sup>14</sup> NTS1 was also found in tumor tissue and was reported to be involved in cancer growth.<sup>15,16</sup> The subtype NTS2 has attracted growing interest because NT(8–13)

derivatives with NTS2 selectivity showed analgesic effects in mice.<sup>17</sup> NTS2 is involved in the modulation of tonic pain sensitivity<sup>18</sup> and is, therefore, regarded as a highly attractive pharmacological target protein. To further elucidate the physiological role of NTS2 and to investigate intermolecular crosstalk between NTS1 and NTS2,<sup>19</sup> highly selective NTS2 ligands will be necessary. As lead compounds, such molecular probes could initiate the development of drug candidates avoiding the risk of tumor promotion associated with the activation of NTS1. Very recently, antipsychotic-like activity was reported for the metabolically stabilized ligand **1** (NT79) showing significant NTS2 preference.<sup>20</sup> According to recent structure–activity relationships (SAR) data, exchange of the parent peptide's *L*-tyrosine unit in position 11 by unnatural *D*-amino acids such as *D*- $\alpha$ -naphthylalanine was accepted by NTS2 but led to a substantial attenuation of NTS1 binding.<sup>17,21,22</sup> These results lead to the suggestion that modifications of both backbone and side chain structure in position 11 might be key to subtype specific receptor recognition. Aiming to discover NTS2 selective ligands, we extended our previous investigations on the discovery and receptor–ligand interactions of neurotensin surrogates.<sup>23–25</sup> On the basis of the

Received: January 4, 2011

Published: March 29, 2011

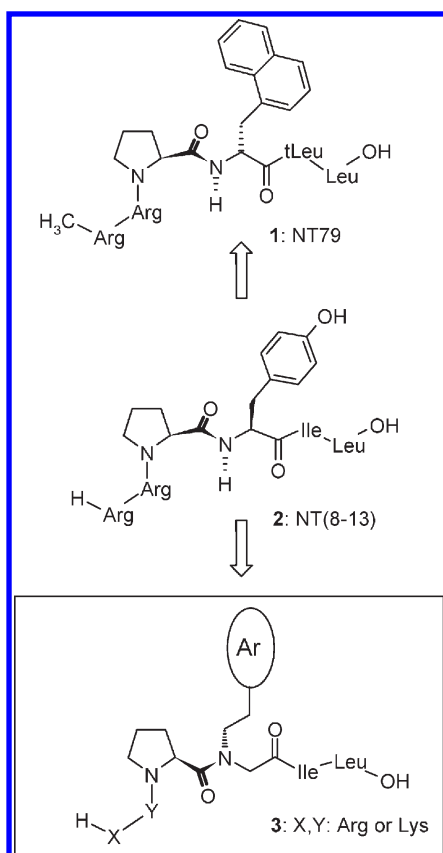
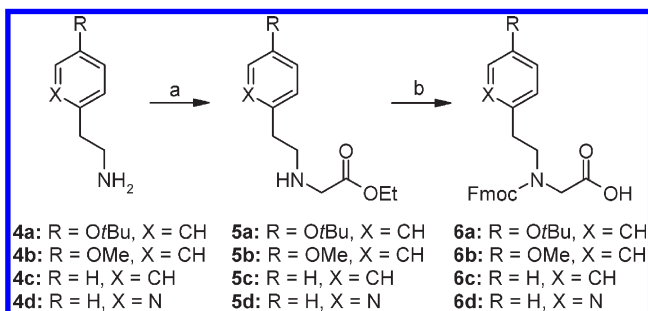


**Figure 1.** Structural modifications leading to the target compounds of type 3.

#### Scheme 1<sup>a</sup>



<sup>a</sup> Reagents and conditions: (a) ethyl bromoacetate, NEt<sub>3</sub>, THF, 0 °C to RT, then RT, 2 h (65–97%); (b) (1) NaOH, MeOH, RT, 30 min, (2) Fmoc-OSu, H<sub>2</sub>O/dioxane, pH 8.5–9.0, 0 °C to RT, then RT, 5 h (63–79%).

above-mentioned studies, an alanine scan and systematic peptide backbone modifications, we herein describe the identification of screening hits and structural modifications leading to the highly potent and NTS2 selective peptide-peptoid hybrids of type 3.

## RESULTS AND DISCUSSION

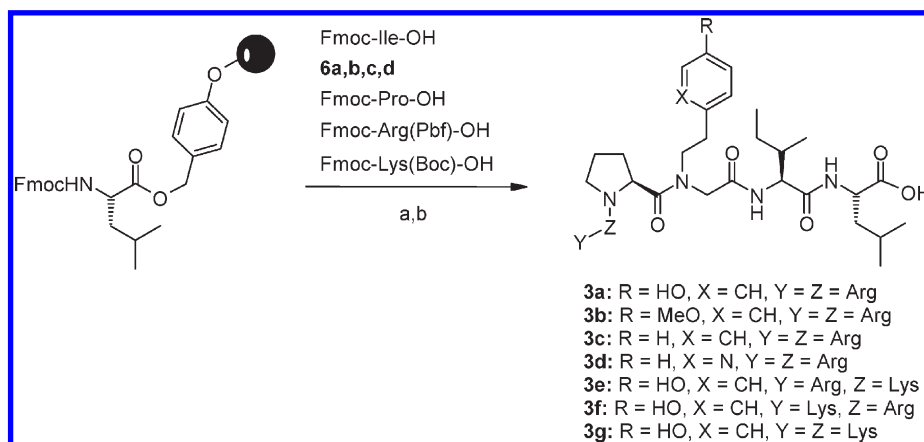
**Chemistry.** Our plan of synthesis of the peptide-peptoid hybrids of type 3 involved the preparation of 9-fluorenylmethyloxycarbonyl (Fmoc)-protected *N*-alkylglycine derivatives and subsequent solid phase supported incorporation of these

building blocks to give the respective peptide-peptoid hybrids. Starting from *O*-*t*-butyl protected tyramine (**4a**)<sup>26</sup> and its structural analogues **4b–4d**, *N*-alkylation was performed with ethyl bromoacetate in presence of triethylamine to furnish the *N*-alkylglycine derivatives **5a–d**.<sup>27–30</sup> Ester hydrolysis and subsequent protection using 9-fluorenylmethyl *N*-hydroxysuccinimidyl carbonate (Fmoc-OSu) gave access to the peptoid building blocks **6a–d** in 48–63% overall yield (Scheme 1).

Solid phase supported peptide synthesis (SPPS) was done starting from Fmoc-leucanyl loaded Wang resin. For the peptides **3a,d**, we followed a conventional protocol, employing piperidine/1,8-diazabicyclo[5.4.0]undec-7-ene (DBU) in dimethylformamide (DMF) to deprotect the Fmoc function. For acylation reactions, we added the respective Fmoc protected amino acids (AA) (5 equiv) and peptoid building blocks (3 equiv) in presence of 2-(1*H*-7-azabenzotriazol-1-yl)-1,1,3,3-tetramethyl uronium hexafluorophosphate (HATU). Peptides **3b,c** were synthesized with the help of microwave irradiation accelerating the Fmoc deprotection and the (benzotriazol-1-yloxy)tripyrrolidinophosphonium hexafluorophosphate (PyBOP) promoted acylation reaction. For the synthesis of the lysine derivatives **3e–g**, we chose PyBOP and 2-(1*H*-6-chlorobenzotriazol-1-yl)-1,1,3,3-tetramethyl uronium hexafluorophosphate (HCTU) promoted, microwave assisted coupling protocols and a HATU induced proline incorporation (Scheme 2).

**Biological Investigations.** To identify subtype selective NTS2 binders, a peptide library was investigated comprising derivatives of NT(8–13) based alanine,<sup>31</sup> *D*-amino acid,<sup>32,33</sup> and homo- $\beta$ -amino acid scans.<sup>25</sup> Additionally, a peptoid scan was performed in comparison to the neurotensin mimetic [<sup>8</sup>Lys, <sup>9</sup>Lys]NT(8–13). Radioligand binding studies were done to evaluate the peptide libraries for NTS1 and NTS2 affinity (Table 1). Binding data were determined utilizing the radioligand [<sup>3</sup>H]neurotensin and stably transfected Chinese hamster ovary (CHO) cells expressing human NTS1 or [<sup>3</sup>H]NT(8–13) and the human NTS2, which was transiently transfected in human embryonic kidney (HEK 239) cells.

Comparison of the selectivity ratios of the reference agents neurotensin, NT(8–13), and [<sup>8</sup>Lys, <sup>9</sup>Lys]NT(8–13), displaying a 2–10 fold preference for NTS1, with the test peptides of the alanine and *D*-amino acid scans, confirmed our initial suggestion that position 11 is crucial to subtype selectivity. Thus, [<sup>11</sup>Ala]NT(8–13) and [<sup>11</sup>*D*-Tyr]NT(8–13) exhibited a 16- and 6.4-fold NTS2 preference. This pattern could be also observed for the peptoid scan when the peptide-peptoid hybrid incorporating an <sup>11</sup>N-Tyr moiety displayed a ratio of *K*<sub>i</sub> values of 30. Thus, formal migration of the 4-hydroxybenzyl side chain from C $\alpha$  to the backbone nitrogen of the reference peptide [<sup>8</sup>Lys, <sup>9</sup>Lys]NT(8–13) led to substantial attenuation of NTS1 binding (NTS1: *K*<sub>i</sub> = 30000 nM). It is noteworthy that structural modifications in position 12 emerged as an alternative strategy. Thus, substitution of <sup>12</sup>Ile by *D*-Ile induced a 19-fold NTS2-selectivity. Moreover, incorporation of homo- $\beta$ -Ile into position 12 led to a selectivity factor of 46 and a *K*<sub>i</sub> value of 5.4 nM for NTS2, which is similar to the data that we received for the reference peptide 1 (*K*<sub>i</sub> = 34 nM, selectivity ratio = 250). We intended to take advantage of efficient synthetic availability of peptide-peptoid hybrids and the thus facilitated practical access to unnatural residues. Starting from the library member H-Lys-Lys-Pro-N-Tyr-Ile-Leu-OH, our SAR studies involved structural modifications in position 8 and 9 back to arginyl units of the parent peptide and structural variation of the hydroxyphenyl

Scheme 2<sup>a</sup>

<sup>a</sup> Reagents and conditions: (a) For **3a,d**: (1) piperidine/DBU/DMF, 2 min, (2) Fmoc-AA, HATU, DIPEA, NMP, RT, 2 h. For **3b,c**: (1) piperidine/DMF,  $\mu$ -wave, (2) Fmoc-AA-OH, PyBOP, DIPEA, HOBt, DMF,  $\mu$ -wave. For **3e**: (1) piperidine/DMF,  $\mu$ -wave, (2) Fmoc-AA-OH, PyBOP, DIPEA, HOBt, DMF,  $\mu$ -wave, except for proline; Fmoc-Pro-OH, HATU, DIPEA,  $\mu$ -wave; For **3f,g**: (1) piperidine/DMF,  $\mu$ -wave, (2) peptide coupling; Fmoc-AA-OH, HCTU, DIPEA,  $\mu$ -wave, except for proline; Fmoc-Pro-OH, HATU, DIPEA,  $\mu$ -wave. (b) TFA/phenol/H<sub>2</sub>O/TIS, RT, 2 h.

function of the peptoid subunit by methoxyphenyl, phenyl, and 2-pyridyl groups. As a compensation of the migration of the attaching point to the backbone nitrogen atom, a homologization was part of our program because we suggested that a higher flexibility of the side chain might allow the ligand to better adapt to the binding pocket of the target receptor NTS2. In fact, the receptor binding data clearly display that the homologization of the side chain substantially increased NTS2 affinity. Thus, the *N*-4-hydroxyphenethyl substituted peptide-peptoid hybrid **3g** displayed excellent NTS2 binding ( $K_i = 4.3$  nM). Interestingly, this gain of affinity was restricted to NTS2 when NTS1 affinity was nearly unchanged by the homologization. This resulted in a 7400-fold selectivity for NTS2 over NTS1. Similar NTS2 affinity (NTS1,  $K_i = 28000$  nM; NTS2,  $K_i = 8.8$  nM) and selectivity was observed for the NT(8–13) analogue **3a**, incorporating two original arginine residues in both positions 8 and 9. Thus, the highly selective NTS2 recognition of the test compound of type **3** goes exclusively back to the peptoid unit in position 11. To examine the relative contribution of both modifications, the migration and the homologization of the tyrosine residue, the peptide H-Arg-Arg-Pro-h-Tyr-Ile-Leu-OH was synthesized and investigated for NTS1 and NTS2 affinity. The data resulted in a  $K_i$  value of 17 nM for NTS2 and a selectivity ratio of 12. Thus, homologization significantly contributes to a favorable NTS2 binding. However, the combination of both manipulations is necessary to generate highly selective NTS2 receptor ligands. Excellent binding and selectivity data were also determined for the [<sup>8</sup>Arg,<sup>9</sup>Lys] and [<sup>8</sup>Lys,<sup>9</sup>Arg] analogues **3e** and **3f**, when the 8-lysiny derivative **3f** showed an unprecedented selectivity ratio of 12000. Thus, both affinity and selectivity ratios of **3a** and **3e–g** significantly exceed those for the NTS2 reference peptide **1**. Compared to the NT(8–13) derived peptoid hybrid **3a**, structural variations of the phenoxy moiety leading to the test compounds **3b–d** resulted in an approximately 2–11 fold decrease of affinity and a significant reduction of selectivity for the para-unsubstituted derivatives **3c,d**, indicating that a hydroxy or methoxy group in para-position of residue 11 is beneficial for the differentiation of a peptidic ligand between NTS2 and NTS1.

To investigate the intrinsic activity of the peptide-peptoid hybrids **3a** and **3e–g** in comparison to the endogenous ligand

neurotensin,<sup>34</sup> a MAPK-driven luciferase reporter gene assay<sup>35,36</sup> was performed by employing transiently transfected HEK 293 cells expressing human NTS1 and NTS2. In this test system, the endogenous ligand neurotensin displayed an inhibition of constitutive MAPK activity, which proved to be strongly increased in NTS2-expressing cells (Supporting Information). Thus, neurotensin behaves as an inverse agonist with an EC<sub>50</sub> value of 110 nM (Figure 2A). In contrast, neurotensin induced an activation of MAPK promoted luciferase expression (EC<sub>50</sub> = 1.6 nM) in NTS1 expressing cell lines (Figure 2C), indicating agonist properties.

Compared to the parent peptide, the <sup>11</sup>Tyr peptoid-peptide hybrids **3a** and **3e–g** showed a superior impact on NTS2 activity. Thus, **3a** and **3g** attenuated constitutive activity of NTS2-expressing HEK 293 cells 2.6–4.6-fold stronger than the endogenous peptide neurotensin (Figure 2A, Table 2), displaying EC<sub>50</sub> values between 480 and 840 nM. To validate that this effect was diagnostic for an NTS2–ligand interaction, constitutive activity of MAPK promoted luciferase expression was attenuated by **3a** and dose dependently regained by addition of the neurotensin receptor antagonist 2-[[[5-(2,6-dimethoxyphenyl)-1-[4-[[[3-(dimethylamino)propyl]methylamino]carbonyl]-2-(1-methylethyl)phenyl]-1*H*-pyrazol-3-yl]carbonyl]amino]-adamantane-2-carboxylic acid (SR142948A)<sup>37</sup> (Figure 2B). As expected from the binding experiments, the NTS2 promoted effects of the test compounds **3a** and **3e–g** proved to be subtype selective over NTS1 ( $E_{\max} < 10\%$  at 10<sup>-5</sup> M) (Table 2, Figure 2C). Thus, the functional assay clearly indicated that the neurotensin mimetics **3a** and **3e–g** act as highly potent and subtype selective inverse agonists that substantially inhibit constitutive activity of NTS2.<sup>38,39</sup>

## CONCLUSION

Aiming to discover NTS2 selective ligands, we herein describe the identification of screening hits and the chemical synthesis of structural variants leading to the highly potent and NTS2 selective peptide-peptoid hybrids of type **3**. The neurotensin mimetics **3a** and **3e–g** incorporating an *N*-(4-hydroxyphenethyl)glycine substructure exhibit single digit nanomolar affinity ( $K_i = 4.3–8.8$  nM) and 1900–12000-fold selectivity over the subtype NTS1. According to functional experiments, the test

**Table 1. Receptor Binding Data of Peptide Library Members and the Lead Modification Products 3a–g in Comparison to the Reference Agents Neurotensin, NT(8–13) (2), 1, and [<sup>8</sup>Lys, <sup>9</sup>Lys]NT(8–13) Employing Human NTS1 and NTS2<sup>a</sup>**

compd	$K_i$ value $\pm$ SEM/SD <sup>b</sup> [nM]		selectivity ratio $K_i$ (NTS1)/ $K_i$ (NTS2)
	hNTS1 <sup>c</sup> [ <sup>3</sup> H]neurotensin	hNTS2 <sup>d</sup> [ <sup>3</sup> H]NT(8–13)	
Alanine Scan			
H-Ala-Arg-Pro-Tyr-Ile-Leu-OH	4.6 $\pm$ 0.57 <sup>b</sup>	56 $\pm$ 10	0.082
H-Arg-Ala-Pro-Tyr-Ile-Leu-OH	11 $\pm$ 4.3 <sup>b</sup>	24 $\pm$ 3.7	0.46
H-Arg-Arg-Ala-Tyr-Ile-Leu-OH	26 $\pm$ 8.2	63 $\pm$ 8.3	0.41
H-Arg-Arg-Pro-Ala-Ile-Leu-OH	1300 $\pm$ 470	83 $\pm$ 10	16
H-Arg-Arg-Pro-Tyr-Ala-Leu-OH	100 $\pm$ 11 <sup>b</sup>	63 $\pm$ 12	1.6
H-Arg-Arg-Pro-Tyr-Ile-Ala-OH	1100 $\pm$ 550 <sup>b</sup>	1300 $\pm$ 290	0.85
D-Amino Acid Scan			
H-D-Arg-Arg-Pro-Tyr-Ile-Leu-OH	0.61 $\pm$ 0.16 <sup>b</sup>	5.4 $\pm$ 1.5 <sup>b</sup>	0.11
H-Arg-D-Arg-Pro-Tyr-Ile-Leu-OH	71 $\pm$ 34 <sup>b</sup>	51 $\pm$ 2.8 <sup>b</sup>	1.4
H-Arg-Arg-D-Pro-Tyr-Ile-Leu-OH	220 $\pm$ 64 <sup>b</sup>	590 $\pm$ 150 <sup>b</sup>	0.37
H-Arg-Arg-Pro-D-Tyr-Ile-Leu-OH	890 $\pm$ 320	140 $\pm$ 45	6.4
H-Arg-Arg-Pro-Tyr-D-Ile-Leu-OH	13000 $\pm$ 710 <sup>b</sup>	690 $\pm$ 100	19
H-Arg-Arg-Pro-Tyr-Ile-D-Leu-OH	1300 $\pm$ 560 <sup>b</sup>	3700 $\pm$ 1200	0.35
Homo- $\beta$ -amino Acid Scan			
H-h $\beta$ -Arg-Arg-Pro-Tyr-Ile-Leu-OH	0.23 $\pm$ 0.047	0.61 $\pm$ 0.13	0.38
H-Arg-h $\beta$ -Arg-Pro-Tyr-Ile-Leu-OH	3.4 $\pm$ 0.99 <sup>b</sup>	16 $\pm$ 2.1 <sup>b</sup>	0.21
H-Arg-Arg-h $\beta$ -Pro-Tyr-Ile-Leu-OH	47 $\pm$ 11	210 $\pm$ 46	0.22
H-Arg-Arg-Pro-h $\beta$ -Tyr-Ile-Leu-OH	8.4 $\pm$ 0.28 <sup>b</sup>	44 $\pm$ 30 <sup>b</sup>	0.19
H-Arg-Arg-Pro-Tyr-h $\beta$ -Ile-Leu-OH	250 $\pm$ 49	5.4 $\pm$ 0.99	46
H-Arg-Arg-Pro-Tyr-Ile-h $\beta$ -Leu-OH	8.4 $\pm$ 1.9	25 $\pm$ 0.0 <sup>b</sup>	0.34
Peptoid Scan			
NLys-Lys-Pro-Tyr-Ile-Leu-OH	1.6 $\pm$ 0.23	0.74 $\pm$ 0.026	2.2
H-Lys-NLys-Pro-Tyr-Ile-Leu-OH	17 $\pm$ 3.4	21 $\pm$ 7.9	0.81
H-Lys-Lys-Pro-N <sup>T</sup> Yr-Ile-Leu-OH	30000 $\pm$ 5900	1000 $\pm$ 280	30
H-Lys-Lys-Pro-Tyr-NIle(1)-Leu-OH <sup>e</sup>	3300 $\pm$ 1000	330 $\pm$ 130	10
H-Lys-Lys-Pro-Tyr-NIle(2)-Leu-OH <sup>e</sup>	3000 $\pm$ 960	1200 $\pm$ 460	2.5
H-Lys-Lys-Pro-Tyr-Ile-NLeu-OH	3700 $\pm$ 1300	1600 $\pm$ 520	2.3
Lead Modification			
3a	28000 $\pm$ 7400	8.8 $\pm$ 1.4	3200
3b	47000 $\pm$ 14000	38 $\pm$ 9.0	1200
3c	2600 $\pm$ 230	20 $\pm$ 5.0	130
3d	10000 $\pm$ 2300	100 $\pm$ 24	100
3e	80000 $\pm$ 20000	6.7 $\pm$ 1.9	12000
3f	8300 $\pm$ 1900	4.4 $\pm$ 1.6	1900
3g	32000 $\pm$ 7000	4.3 $\pm$ 0.63	7400
H-Arg-Arg-Pro-h-Tyr-Ile-Leu-OH	210 $\pm$ 57 <sup>b</sup>	17 $\pm$ 2.1 <sup>b</sup>	12
Reference Agents			
neurotensin	0.59 $\pm$ 0.16 <sup>f</sup>	4.9 $\pm$ 0.37	0.12
NT(8–13) (2)	0.24 $\pm$ 0.024	1.2 $\pm$ 0.17 <sup>f</sup>	0.20
1	8500 $\pm$ 2300	34 $\pm$ 9.5	250
H-Lys-Lys-Pro-Tyr-Ile-Leu-OH	2.7 $\pm$ 0.42 <sup>b</sup>	6.1 $\pm$ 0.71 <sup>b</sup>	0.44

<sup>a</sup>  $K_i$  values  $\pm$  SEM are the means of 3–16 individual experiments each done in triplicate. <sup>b</sup>  $K_i$  values  $\pm$  SD derived from two experiments. <sup>c</sup> Membranes from CHO cells stably expressing human NTS1. <sup>d</sup> Homogenates from HEK cells transiently expressing hNTS2. <sup>e</sup> Due to the application of (RS)-2-butylamine for the peptoid synthesis, we obtained two separable isomers of the respective Ile-peptoid, which were HPLC separated. <sup>f</sup>  $K_D$  values  $\pm$  SEM.

compounds 3a and 3e–g displayed an inhibition of constitutive MAPK activity exceeding 2.6–4.6 times the inverse agonist activity of the endogenous ligand neurotensin. As lead

compounds, molecular probes of type 3 will initiate the development of drug candidates avoiding the risk of tumor promotion associated with the activation of NTS1. The objective of this

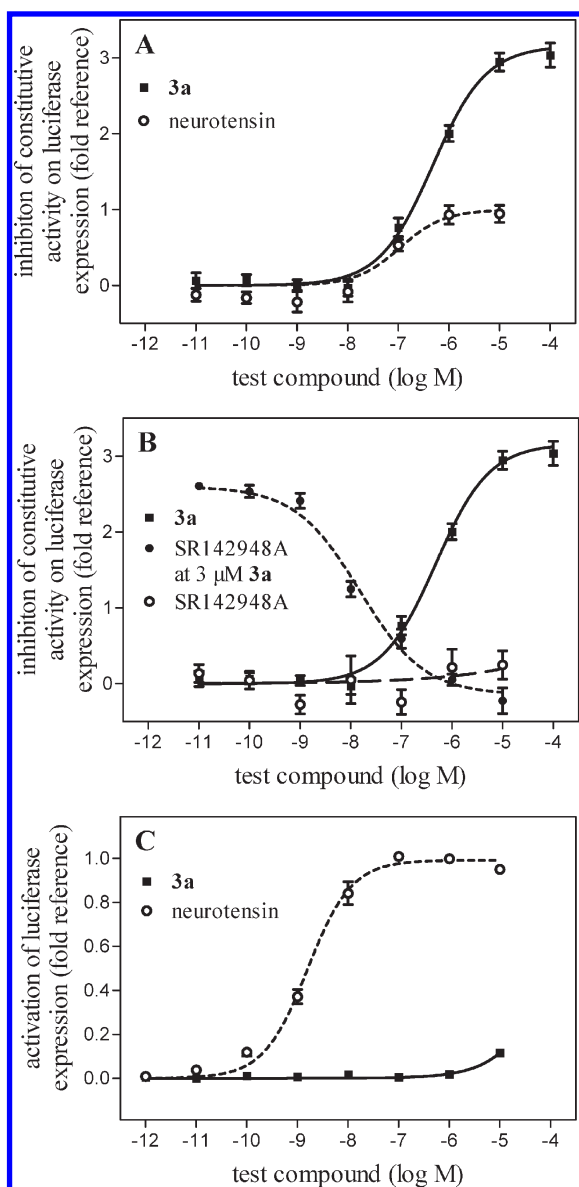


**Figure 2.** Functional activity of the test compound 3a compared to the reference NT employing a MAPK-driven reporter gene assay in hNTS1- and hNTS2-expressing HEK 293 cells. (A) Inhibition of the constitutive activity on luciferase expression in hNTS2 expressing cells as a measure of intrinsic activity of 3a and NT. (B) Dose dependent attenuation of the intrinsic effect of 3  $\mu$ M 3a mediated by the antagonist SR142948A as a diagnostic measure of NTS2 specific activation. (C) Activation of luciferase expression in hNTS1 expressing cells mediated by 3a in comparison to NT. Mean curves of 7–11 pooled, independent experiments each done in triplicate.

work was to discover NTS2 selective ligands. We anticipate that the peptoid moiety in position 11 of final products of type 3 will be advantageous for in vivo stability.<sup>40–42</sup> Because our molecular probes still contain peptidic partial structures, further chemical manipulations will be necessary to evaluate pharmacokinetic profiles and to achieve oral bioavailability.

## EXPERIMENTAL SECTION

**Chemistry.** Reagents and dry solvents were obtained from commercial sources and were used as received. Reactions were conducted

**Table 2.** Functional Activity of 3a, 3e–g, the Reference Neutrotensin, and the Antagonist SR142948A Derived from the Modulation of MAPK-Driven Luciferase Activity in hNTS1 and hNTS2 Expressing Cells

compd	hNTS1		hNTS2	
	EC <sub>50</sub> [nM] <sup>a</sup>	E <sub>max</sub> <sup>b</sup>	EC <sub>50</sub> [nM] <sup>a</sup>	E <sub>max</sub> <sup>b</sup>
3a		0.12	480	3.2
3e		0.07	840	2.6
3f		0	690	4.6
3g		0	590	3.1
SR142948A		0		0
neurotensin	1.6	1.0	110	1.0

<sup>a</sup>EC<sub>50</sub> values in [nM] derived from the mean curves of 3–11 independent experiments each done in triplicate. <sup>b</sup>Ligand efficacy expressed as E<sub>max</sub> in [fold reference].

under dry N<sub>2</sub>. Evaporations of product solutions were done in vacuo with a rotary evaporator. Column chromatography was performed using 60  $\mu$ m silica gel. For thin layer chromatography (TLC), silica gel 60  $\mu$ m plates were used (ultraviolet (UV), I<sub>2</sub> or ninhydrin detection). Melting temperatures are uncorrected. Infrared (IR) spectra were registered from a thin film on a NaCl crystal. Nuclear magnetic resonance (NMR) data were acquired with the help of a 360 MHz (if not otherwise stated) or a 600 MHz spectrometer, if not stated otherwise in CDCl<sub>3</sub>; <sup>13</sup>C NMR spectra were recorded at 90 MHz if not stated otherwise in CDCl<sub>3</sub>. Chemical shifts are given in  $\delta$  relative to tetramethylsilane (TMS) in parts per million (ppm). Mass spectra were acquired using electronic ionization (EI), atmospheric pressure chemical ionization (APCI) or electron spray ionization (ESI) techniques. ESI-ToF high mass accuracy and resolution experiments were performed on a Bruker maXis MS (Bruker Daltonics, Bremen, Germany) in the laboratory of the Chair of Bioinorganic Chemistry (Prof. Dr. Ivana Ivanović-Burmazović), FAU. CHN analyses were conducted in the analytical laboratory of the Division of Organic Chemistry, FAU. High performance liquid chromatography (HPLC) analysis revealed a purity >95% for all SAR compounds.

**N-[2-(*tert*-Butyloxyphenyl)ethyl]glycine Ethyl Ester<sup>27,28</sup> (5a).** Ethyl bromoacetate (448.0 mg, 2.68 mmol), 2-(4-*tert*-butyloxyphenyl)ethylamine (4a, 569.0 mg, 2.95 mmol),<sup>26a</sup> and triethylamine (0.74 mL, 5.36 mmol) were dissolved in tetrahydrofuran (THF) (4 mL) at 0 °C and then stirred at room temperature (RT) for 4 h. The mixture was filtered and the residue washed with THF. The filtrate was concentrated in vacuo, and the residue was purified by flash column chromatography (hexane/ethyl acetate gradient 9:1  $\rightarrow$  7:3  $\rightarrow$  5:5) to afford 5a (594.0 mg, 79%) as a colorless oil. IR (film, NaCl) 3451, 3334, 1739 cm<sup>-1</sup>. <sup>1</sup>H NMR  $\delta$  1.25 (t, *J* = 7.1 Hz, 3H), 1.32 (s, 9H), 1.64 (brs, 1H), 2.77 (m, 2H), 2.86 (m, 2H), 3.41 (s, 2H), 4.17 (q, *J* = 7.1 Hz, 2H), 6.91 (m, 2H), 7.01 (m, 2H). <sup>13</sup>C NMR (90 MHz)  $\delta$  14.2, 29.0, 35.8, 50.8, 51.0, 60.7, 78.2, 124.2, 129.0, 134.5, 153.7, 172.3. APCI-MS 280 [M + H]<sup>+</sup>.

**N-(9-Fluorenylmethoxycarbonyl)-N-[2-(4-*tert*-butyloxyphenyl)ethyl]glycine (6a).**<sup>27,28</sup> To a solution of N-[2-(4-*tert*-butyloxyphenyl)ethyl]glycine ethyl ester (5a, 365.5 mg, 1.28 mmol) in MeOH (4 mL), 4N NaOH (0.64 mL, 2.56 mmol) was added and stirring was performed for 30 min. The mixture was concentrated in vacuo, and then water (4 mL) was added and the pH was adjusted to 9.0–9.5 by employing 2N HCl. Subsequently, the mixture was cooled to 0 °C and a solution of Fmoc-OSu (451.7 mg, 1.34 mmol) in dioxan (8 mL) was added. The pH was readjusted to 9.0–9.5, and stirring at RT was performed for 5 h. After addition of water, the solution was extracted with diethylether, and the organic layer was discarded. Thereafter, the

aqueous layer was acidified to pH 7.5–8.0 and extracted with ethyl acetate. The combined organic layers were dried using  $\text{Na}_2\text{SO}_4$  and concentrated in vacuo. Recrystallization (diethylether/hexane) afforded **6a** (400.0 mg, 66%) as a white solid, melting point (mp) 123–124 °C. IR (film, NaCl) 3413, 1697  $\text{cm}^{-1}$ .  $^1\text{H}$  NMR (two rotamers were observed)  $\delta$  1.31 (s, 9H), 2.51 and 2.78 (2  $\times$  t, each  $J = 7.1$  Hz, 2H), 3.30 and 3.49 (2  $\times$  t, each  $J = 7.1$  Hz, 2H), 3.69 and 3.81 (2  $\times$  s, 2H), 4.21 (m, 1H), 4.45 and 4.57 (2  $\times$  m, 2H), 6.81–6.85 (m, 2H), 6.89 and 7.03 (2  $\times$  m, 2H), 7.26–7.39 (m, 4H), 7.51 and 7.58 (2  $\times$  d, each  $J = 7.4$  Hz, 2H), 7.72 (d,  $J = 7.4$  Hz, 2H).  $^{13}\text{C}$  NMR (90 MHz)  $\delta$  29.3, 33.7, 34.0, 47.2, 47.3, 49.0, 49.5, 50.3, 50.8, 67.2, 67.5, 77.2, 78.1, 119.9, 120.0, 124.3, 124.4, 124.7, 124.8, 127.0, 127.1, 127.6, 127.7, 129.0, 129.1, 133.2, 133.6, 141.3, 141.4, 143.8, 153.8, 155.6, 156.6, 174.5, 174.7. APCI-MS 474  $[\text{M} + \text{H}]^+$ . Anal. Calcd for  $\text{C}_{29}\text{H}_{31}\text{NO}_5$  (351.40): C, 73.55; H, 6.60; N, 2.96. Found: C, 73.14; H, 6.22; N, 2.65.

**Synthesis of the Peptide–Peptoid Hybrids.** The peptide synthesis was done according to standard protocols as described below. The synthesis was performed starting from commercially available Fmoc-Leu-Wang resin.  $\alpha$ -Amino acids were incorporated as their commercially available derivatives: Fmoc-Ile-OH, Fmoc-Pro-OH, and Fmoc-Arg(Pbf)-OH. Elongation of the peptide chain was done by repetitive cycles of Fmoc deprotection either without (elongation method 1) or with the help of microwave irradiation (elongation method 2 and 3) and subsequent coupling of the AA derivative. After the last acylation step, the *N*-terminal Fmoc-residue was deprotected, the resin was 10  $\times$  rinsed with  $\text{CH}_2\text{Cl}_2$  and dried in vacuo. The cleavage from the resin was performed using a mixture of trifluoroacetic acid (TFA)/phenol/ $\text{H}_2\text{O}$ /triisopropylsilane (TIS) 88:5:5:2 for 2 h, followed by a filtration of the resin. After evaporation of the solvent in vacuo and precipitation in *t*-butylmethylether, the crude peptides were purified using preparative RP-HPLC: Agilent 1100 preparative series, column Zorbax Eclipse XDB-C8, 21.2 mm  $\times$  150 mm, 5  $\mu\text{m}$  particles [C8], employing solvent systems, linear gradient and flow rate [FR] as specified below or ZORBAX 300SB-C18, 21.2 mm  $\times$  250 mm, 7  $\mu\text{m}$  column [C18] employing solvent systems, linear gradient and flow rate [FR] as specified below.

After the separation, the peptides were lyophilized and peptide purity and identity were assessed by analytical HPLC (Agilent 1100 analytical series, equipped with QuatPump and VWD detector; column Zorbax Eclipse XDB-C8 analytical column, 4.6 mm  $\times$  150 mm, 5  $\mu\text{m}$ , flow rate 0.5 mL/min) coupled to a Bruker Esquire 2000 mass detector equipped with an ESI-trap. System 1 (S1):  $x$ – $y$  %  $\text{CH}_3\text{OH}$  in  $\text{H}_2\text{O}$  + 0.1%  $\text{HCO}_2\text{H}$  in 18 min (S1A: 10–40% in 18 min, 40–95% in 2 min, 95–95% in 2 min, S1B 10–55%), system 2 (S2):  $x$ – $y$  %  $\text{CH}_3\text{CN}$  in  $\text{H}_2\text{O}$  + 0.1%  $\text{HCO}_2\text{H}$  in 26 min (S2A: 3–40%, S2B 3–20%).

**Elongation Method 1 (EM1).** Fmoc deprotection: the resin was treated 5  $\times$  with 2% DBU/2% piperidine in DMF for 2 min and rinsed with  $\text{CH}_2\text{Cl}_2$  (10  $\times$ ). HATU (3–5 equiv) and the carboxylic acids (3–5 equiv) were dissolved in *N*-methylpyrrolidone (NMP) (least volume possible). After addition of diisopropylethylamine (DIPEA) (6–10 equiv), the mixture was added to the resin and agitated for 8–16 h, followed by several  $\text{CH}_2\text{Cl}_2$  washes. For the introduction of the peptoid moiety, 3 equiv of the building blocks was employed. Fmoc-Pro-OH and the first Fmoc-Arg(Pbf)-OH were attached using a double coupling, initially employing 5 equiv, then 3 equiv of the carboxylic acid derivative. If possible, complete acylation was monitored with the help of the Kaiser Test. When the test indicated incomplete coupling, the procedure was repeated.

**Elongation Method 2 (EM2).** Microwave assisted (Discover microwave oven, CEM Corp.) peptide synthesis was carried out in silanized glass tubes loosely sealed with a silicon septum. Remark: the development of overpressure was avoided by using DMF as the solvent and intermittent cooling. Fmoc deprotection: the resin was treated 1  $\times$  with 20% piperidine in DMF (microwave irradiation: 5  $\times$  5 s, 100 W),

followed by washings with DMF (5  $\times$ ). Peptide coupling was done employing 5 equiv of each Fmoc-AA/PyBOP/DIPEA and 7.5 equiv 1-hydroxybenzotriazole (HOBt), dissolved in a minimum amount of DMF (irradiation: 15  $\times$  10 s, 50 W). In between each irradiation step, cooling of the reaction mixture to a temperature of  $-10$  °C was achieved by sufficient agitation in an ethanol–ice bath.

**Elongation Method 3 (EM3).** Microwave irradiation was done as described for EM2. For the synthesis of **3e**, peptide coupling was performed employing 5 equiv of the corresponding Fmoc-AA/PyBOP/DIPEA and 7.5 equiv HOBt, the peptoid (3 equiv) was coupled with 3 equiv PyBOP/DIPEA and 4.5 equiv HOBt in DMF. For the synthesis of **3f,g**, 5 equiv of the each Fmoc-AA/HCTU and 10 equiv DIPEA (for the peptoid building block 3/3/6 equiv) in DMF were applied. Fmoc-Pro-OH (5 equiv) was routinely coupled 2  $\times$  with HATU (5 equiv) and DIPEA (10 equiv) in DMF.

**[ $^{11}\text{N}$ -(2-(4-Hydroxyphenyl)ethyl)-Gly]NT(8–13) (3a).** The peptide–peptoid hybrid was synthesized according to EM1. Purification [C18]: eluent: 0.1% TFA in acetonitrile (A) and 0.1% TFA in  $\text{H}_2\text{O}$  (B) applying a linear gradient starting from 5% A in 95% B to 35% A in 65% B in 14.0 min, FR 21.0 mL/min,  $t_r$  12.6 min. Purity: S1B, 98.0% ( $t_r$ : 13.7 min); S2A, 98.0% ( $t_r$ : 14.7 min).  $[\text{M} + \text{H}]^+$ : calcd, 831.5; found, 831.6. HRESI-TOF: calcd for  $\text{C}_{39}\text{H}_{67}\text{N}_{12}\text{O}_8$ , 831.5205; found, 831.5192.

**[ $^9\text{Lys}$ ,  $^{11}\text{N}$ -(2-(4-Hydroxyphenyl)ethyl)-Gly]NT(8–13) (3e).** The peptide was synthesized according to EM3. Purification [C8]: MeOH (A) and 0.1%  $\text{HCO}_2\text{H}$  in  $\text{H}_2\text{O}$  (B) applying a linear gradient starting from 10% A in 90% B to 50% A in 50% B in 18.0 min. FR: 10.0 mL/min.  $t_r$ : 8.8 min. Purity: S1B >99% ( $t_r$ : 13.3 min); S2A 99% ( $t_r$ : 14.8 min).  $[\text{M} + \text{H}]^+$ : calcd, 803.5; found, 803.6.

**[ $^8\text{Lys}$ ,  $^{11}\text{N}$ -(2-(4-Hydroxyphenyl)ethyl)-Gly]NT(8–13) (3f).** The peptide was synthesized according to EM3. Purification [C8]: MeOH (A) and 0.1%  $\text{HCO}_2\text{H}$  in  $\text{H}_2\text{O}$  (B) applying a linear gradient starting from 10% A in 90% B to 50% A in 50% B in 18.0 min. FR: 10.0 mL/min.  $t_r$ : 9.3 min. purity: S1B, 98.6% ( $t_r$ : 14.0 min); S2A, 96.8% ( $t_r$ : 15.4 min).  $[\text{M} + \text{H}]^+$ : calcd, 803.5; found, 803.6.

**[ $^8\text{Lys}$ ,  $^9\text{Lys}$ ,  $^{11}\text{N}$ -(2-(4-Hydroxyphenyl)ethyl)-Gly]NT(8–13) (3g).** The peptide was synthesized according to EM3. Purification [C8]: MeOH (A) and 0.1%  $\text{HCO}_2\text{H}$  in  $\text{H}_2\text{O}$  (B) applying a linear gradient starting from 10% A in 90% B to 50% A in 50% B in 18.0 min. FR: 10.0 mL/min.  $t_r$ : 8.9 min. Purity: S1B 96.9% ( $t_r$ : 12.8 min); S2A 95.8% ( $t_r$ : 14.2 min).  $[\text{M} + \text{H}]^+$ : calcd, 775.5; found, 775.6.

**Cloning and Transfection.** The hNTS1 and hNTS2 cDNA was purchased from the UMR cDNA Resource Center subcloned into a pcDNA3.1(+) eukaryotic expression vector. To create a cell line stably expressing hNTS1 the pcDNA3.1 hNTS1 expression vector was used to clone CHO FRT cells (Invitrogen, Darmstadt, GE). Cells were grown in DMEM-F12 supplemented with 10% fetal bovine serum (FBS), 2 mM L-glutamine, 1% Pen-Strep (all from Invitrogen), and 400  $\mu\text{g}/\text{mL}$  hygromycin B (Calbiochem Merck Chemicals, Nottingham, UK). For receptor binding experiments with NTS2, HEK 293 cells were transiently transfected according to the calcium phosphate precipitation method.<sup>43</sup> For the reporter-gene assay on functional activity of NTS1 and NTS2 HEK 293 cells were transiently transfected with the lipofectine method using the *TransIT*-293 transfection reagent (Mirus Bio Corporation, Madison, WI). In brief, transient transfection was done with HEK 293 cells, which were maintained in DMEM-F12 supplemented with 10% FBS, 2 mM L-glutamine, and 1% Pen-Strep and kept in a humid atmosphere at 37 °C and 5%  $\text{CO}_2$ . For the calcium phosphate precipitation method, 30  $\mu\text{g}$  of pcDNA3.1 hNTS2 was added to each 15 cm dish, cells were grown for 48 h and harvested and worked up as described previously.<sup>44</sup> For the reporter-gene assay HEK 293 cells were grown in 10 cm dishes to about 60% confluency and lipofectine transfection was done by adding a mixture of 6  $\mu\text{g}$  gene of interest (pcDNA3.1 hNTS1 or pcDNA3.1 hNTS2), 5  $\mu\text{g}$  pFR-Luc reporter

plasmid, and 0.5  $\mu\text{g}$  pFA2-Elk1 trans-activator plasmid (PathDetect Elk1 Trans-Reporting System, Stratagene, Santa Clara, CA) to the cells.

**Receptor Binding Experiments.** Receptor binding data were determined according to protocols as described previously.<sup>45</sup> In detail, hNTR1 binding was measured using homogenats of membranes from CHO cells stably expressing human NTR1 at a final concentration of 2  $\mu\text{g}$ /well and the radioligand [<sup>3</sup>H]neurotensin (specific activity 116 Ci/mmol; PerkinElmer, Rodgau, Germany) at a concentration of 0.5 nM.<sup>46</sup> Specific binding of the radioligand was determined at a  $K_D$  value of  $0.59 \pm 0.16$  nM and a  $B_{\text{max}}$  of 1150–7290 fmol/mg protein. Unspecific binding was determined in the presence of 10  $\mu\text{M}$  neurotensin. NTS2 binding was done using homogenats of membranes from HEK 293, which were transiently transfected with the pcDNA3.1 vector containing the human NTS2 gene (UMR) by the calcium phosphate method.<sup>43</sup> Membranes were incubated at a final concentration of 20  $\mu\text{g}$ /well together with 0.5 nM of [<sup>3</sup>H]NT(8–13) (specific activity 136 Ci/mmol; custom synthesis of [leucine-<sup>3</sup>H]NT(8–13) by GE Healthcare, Freiburg, Germany) at a  $K_D$  value of  $1.2 \pm 0.17$  nM and a  $B_{\text{max}}$  of 325–2560 fmol/mg protein. Specific binding of the radioligand was determined at a  $K_D$  value of 0.47–0.54 nM and a  $B_{\text{max}}$  of 5050–7030 fmol/mg protein. Unspecific binding was determined in the presence of 10  $\mu\text{M}$  NT(8–13) and the protein concentration was generally established by the method of Lowry using bovine serum albumin as standard.<sup>47</sup>

**Luciferase Reporter-Genes Assay.** The luciferase reporter gene assay was performed according to the manufacturer's instructions (PathDetect Elk1 Trans-Reporting System, Stratagene, USA). Briefly, HEK 293 cells were transfected with the *TransIT*-293 transfection reagent (Mirus Bio Corporation, Madison, WI). Twenty-four hours after transfection, cells were trypsinized and washed once to remove FBS. Cells were resuspended in DMEM-F12 supplemented with 1% FBS, 2 mM L-glutamine, and 1% Pen-Strep and seeded into white half area 96-well plates (50000 cells/well). The test compounds were added at the indicated concentrations at a final volume of 50  $\mu\text{L}$  and incubated for 24 h at 37 °C and 5% CO<sub>2</sub>. To quantify an increase in luciferase expression, 50  $\mu\text{L}$  of Bright-Glo reagent (Promega, Mannheim, Germany) was added to each well. After 2 min of incubation at RT and constant agitation to achieve complete cell lysis, luminescence was measured with a multiplate reader (Viktor<sup>3</sup>V, Perkin-Elmer, Rodgau Germany).

**Data Analysis.** Data analysis of the competition curves from the radioligand binding experiments was accomplished by nonlinear regression analysis using the algorithms in PRISM (GraphPad Software, San Diego, CA). EC<sub>50</sub> values derived from the resulting dose response curves were transformed into the corresponding  $K_i$  values utilizing the equation of Cheng and Prusoff.<sup>48</sup>

Data analysis of the reporter-gene assay started when transforming the displayed luminescence values which were given as relative luminescence units (RLU) into normalized data. For NTS1 activation the efficacy ( $E_{\text{max}}$ ) of the test compound was expressed as fold effect of the reference NT. For hNTS2 expressing cells the basal constitutive activity (see Supporting Information) was defined as difference of RLU compared to mock transfected cells expressing neither hNTS1 nor hNTS2. The maximum attenuating effect of NT on RLU was defined as 100% and the effects of the test compounds were set as fold of NT. The resulting curves were analyzed by nonlinear regression analysis to determine EC<sub>50</sub> values representing the concentration corresponding to 50% of maximal efficacy.

## ■ ASSOCIATED CONTENT

**S Supporting Information.** Experimental details for **3b–d**, **5b–d**, and **6b–d**, NMR spectra of **6b**, **6d**, and **3a**, constitutive activity of NTS2, and details with respect to the functional

experiments are presented. This material is available free of charge via the Internet at <http://pubs.acs.org>.

## ■ AUTHOR INFORMATION

### Corresponding Author

\*Phone: +49 9131 85-29383. Fax: +49 9131 85-22585. E-mail: [peter.gmeiner@medchem.uni-erlangen.de](mailto:peter.gmeiner@medchem.uni-erlangen.de).

## ■ ACKNOWLEDGMENT

This work was supported by the Deutsche Forschungsgemeinschaft (DFG). Iris Torres is acknowledged for skilful technical assistance. We thank Prof. Ivana Ivanović-Burmazović and Leanne Nye for high resolution ESI-TOF mass spectra. M.P. thanks the Universität Bayern e.V. for a Ph.D. grant.

## ■ ABBREVIATIONS USED

NTS1, neurotensin receptor 1; NTS2, neurotensin receptor 2; NTS3, neurotensin receptor 3; GPCR, G-protein coupled receptor; CNS, central nervous system; SAR, structure–activity relationships; AA, amino acid; CHO, Chinese hamster ovary; HEK, human embryonic kidney; SPPS, solid phase peptide synthesis; Fmoc, 9-fluorenylmethoxycarbonyl; THF, tetrahydrofuran; HATU, 2-(1*H*-7-azabenzotriazol-1-yl)-1,1,3,3-tetramethyluronium hexafluorophosphate; PyBOP, (benzotriazol-1-yloxy)-tripyrrolidinophosphonium hexafluorophosphate; HCTU, 2-(1*H*-6-chlorobenzotriazol-1-yl)-1,1,3,3-tetramethyluronium hexafluorophosphate; HPLC, high performance liquid chromatography; Pbf, 2,2,4,6,7-pentamethyldihydrobenzofuran-5-sulfonyl; DBU, 1,8-diazabicyclo[5.4.0]undec-7-ene; Boc, *tert*-butyloxycarbonyl; HOBt, 1-hydroxybenzotriazole; NMP, *N*-methylpyrrolidone; DMF, dimethylformamide; DIPEA, diisopropylethylamine; TFA, trifluoroacetic acid; TIS, triisopropylsilane; MAPK, mitogen-activated protein kinase; TLC, thin layer chromatography; IR, infrared; UV, ultraviolet; NMR, nuclear magnetic resonance; TMS, tetramethylsilane; EI-MS, electron ionization mass spectroscopy; APCI, atmospheric pressure chemical ionization; ESI, electron spray ionization; RT, room temperature; MeOH, methanol; mp, melting point; CHN, combustion/elemental analysis; FBS, fetal bovine serum; RLU, relative luminescence units

## ■ REFERENCES

- (1) Carraway, R.; Leeman, S. E. Characterization of Radioimmunoassayable Neurotensin in the Rat. Its Differential Distribution in the Central Nervous System, Small Intestine, and Stomach. *J. Biol. Chem.* **1976**, *251*, 7045–7052.
- (2) Kitabgi, P.; Carraway, R.; Leeman, S. E. Isolation of a Tridecapeptide from Bovine Intestinal Tissue and its Partial Characterization as Neurotensin. *J. Biol. Chem.* **1976**, *251*, 7053–7058.
- (3) Bissette, G.; Nemeroff, C. B.; Loosen, P. T.; Prange, P. T., Jr.; Lipton, M. A. Hypothermia and Intolerance to Cold Induced by Intracisternal Administration of the Hypothalamic Peptide Neurotensin. *Nature* **1976**, *262*, 607–609.
- (4) Clineschmidt, B. V.; McGuffin, J. C.; Bunting, P. B. Neurotensin: Antinociceptive Action in Rodents. *Eur. J. Pharmacol.* **1979**, *54*, 129–139.
- (5) Skoog, K. M.; Cain, S. T.; Nemeroff, C. B. Centrally Administered Neurotensin Suppresses Locomotor Hyperactivity Induced by *D*-Amphetamine but not by Scopolamine or Caffeine. *Neuropharmacology* **1985**, *25*, 777–782.

- (6) St-Pierre, S.; Lalonde, J. M.; Gendron, M.; Quirion, R.; Regoli, D.; Rioux, F. Synthesis of Peptides by the Solid-Phase Method. 6. Neurotensin, Fragments, and Analogues. *J. Med. Chem.* **1981**, *24*, 370–376.
- (7) (a) Hughes, F. M., Jr.; Shaner, B. E.; May, L. A.; Zotian, L.; Brower, J. O.; Woods, R. J.; Cash, M.; Morrow, D.; Massa, F.; Mazella, J.; Dix, T. A. Identification and Functional Characterization of a Stable, Centrally Active Derivative of the Neurotensin (8–13) Fragment as a Potential First-in-Class Analgesic. *J. Med. Chem.* **2010**, *53*, 4623–4632. (b) Rossi, G. C.; Matulonis, J. E.; Richelson, E.; Barbut, D.; Pasternak, G. W. Systemically and Topically Active Antinociceptive Neurotensin Compounds. *J. Pharmacol. Exp. Ther.* **2010**, *334*, 1075–1079.
- (8) (a) Maes, V.; Garcia-Garayoa, E.; Bläuenstein, P.; Tourwe, D. Novel <sup>99m</sup>Tc-Labeled Neurotensin Analogues with Optimized Biodistribution Properties. *J. Med. Chem.* **2006**, *49*, 1833–1836. (b) Nock, B. A.; Nikolopoulou, A.; Reubi, J.-C.; Maes, V.; Conrath, P.; Tourwe, D.; Maina, T. Toward Stable N<sub>4</sub>-Modified Neurotensins for NTS1-Receptor-Targeted Tumor Imaging with <sup>99m</sup>Tc. *J. Med. Chem.* **2006**, *49*, 4767–4776.
- (9) Tanaka, K.; Masu, M.; Nakanishi, S. Structure and Functional Expression of the Cloned Rat Neurotensin Receptor. *Neuron* **1990**, *4*, 847–854.
- (10) Vita, N.; Laurent, P.; Lefort, S.; Chalon, P.; Dumont, X.; Kaghad, M.; Gully, D.; Le Fur, G.; Ferrara, P.; Caput, D. Cloning and Expression of a Complementary DNA Encoding a High Affinity Human Neurotensin Receptor. *FEBS Lett.* **1993**, *317*, 139–142.
- (11) Chalon, P.; Vita, N.; Kaghad, M.; Guillemot, M.; Bonnin, J.; Delpech, B.; Le Fur, G.; Ferrara, P.; Caput, D. Molecular Cloning of a Levocabastine-Sensitive Neurotensin Binding Site. *FEBS Lett.* **1996**, *386*, 91–94.
- (12) Mazella, J.; Botto, J. M.; Guillemare, E.; Coppola, T.; Sarret, P.; Vincent, J. P. Structure, Functional Expression, and Cerebral Localization of the Levocabastine-Sensitive Neurotensin/Neuromedin N Receptor from Mouse Brain. *J. Neurosci.* **1996**, *16*, 5613–5620.
- (13) Mazella, J.; Nicole Zsürger, N.; Navarro, V.; Chabry, J. I.; Kaghad, M.; Caput, D.; Ferrara, P.; Vita, N.; Gully, D.; Jean-Pierre Maffrand, J.-P.; Jean-Pierre Vincent, J.-P. The 100 kDa Neurotensin Receptor is gp95/Sortilin, a non-G-Protein-Coupled Receptor. *J. Biol. Chem.* **1998**, *273*, 26273–26276.
- (14) Alifano, M.; Souazé, F.; Dupouy, S.; Camilleri-Broët, S.; Younes, M.; Ahmed-Zaid, S.-M.; Takahashi, T.; Cancellieri, A.; Damiani, S.; Boaron, M.; Broët, P.; Miller, L. D.; Gespach, C.; Regnard, J. F.; Forgez, P. Neurotensin Receptor 1 Determines the Outcome of Non-Small Cell Lung Cancer. *Clin. Cancer Res.* **2010**, *16*, 4401–4410.
- (15) Caraway, R. E.; Plona, A. M. Involvement of Neurotensin in Cancer Growth: Evidence, Mechanisms and Development of Diagnostic Tools. *Peptides* **2006**, *27*, 2445–2460 and references cited therein.
- (16) Myers, R. M.; Shearman, J. W.; Kitching, M. O.; Ramos-Montoya, A.; Neal, D. E.; Ley, S. V. Cancer, Chemistry, and the Cell: Molecules that Interact with the Neurotensin Receptors. *ACS Chem. Biol.* **2009**, *4*, 503–525.
- (17) Dubuc, I.; Sarret, P.; Labbé-Juillié, C.; Botto, J. M.; Honore, E.; Bourdel, E.; Martinez, J.; Costentin, J.; Jean-Pierre Vincent, J.-P.; Patrick Kitabgi, P.; Mazella, J. Identification of the Receptor Subtype Involved in the Analgesic Effect of Neurotensin. *J. Neurosci.* **1999**, *19*, 503–510.
- (18) Roussy, G.; Dansereau, M.-A.; Baudisson, S.; Ezzoubaa, F.; Belleville, K.; Beaudet, N.; Martinez, J.; Richelson, E.; Sarret, P. Evidence for a Role of NTS2 Receptors in the Modulation of Tonic Pain Sensitivity. *Mol. Pain* **2009**, *5*, 38.
- (19) Hwang, J. R.; Baek, M. W.; Sim, J.; Choi, H.-S.; Han, J. M.; Kim, Y. L.; Hwang, J.-L.; Kwon, H. B.; Beaudet, N.; Sarret, P.; Seong, J. Y. Intermolecular Cross-Talk between NTR1 and NTR2 Neurotensin Receptor Promotes Intracellular Sequestration and Functional Inhibition of NTR1 Receptors. *Biochem. Biophys. Res. Commun.* **2010**, *391*, 1007–1013.
- (20) Boules, M.; Liang, Y.; Briody, S.; Miura, T.; Fauq, I.; Oliveros, A.; Wilson, M.; Khaniyev, S.; Williams, K.; Li, Z.; Qi, Y.; Katovich, M.; Richelson, E. NT79: a Novel Neurotensin Analog with Selective Behavioural Effects. *Brain. Res.* **2010**, *1308*, 35–46.
- (21) For example, see: Tyler, B. M.; Douglas, C. L.; Fauq, A.; Pang, Y.-P.; Stewart, J. A.; Cusack, B.; McCormick, D. J.; Richelson, E. In Vitro Binding and CNS Effects of Novel Neurotensin Agonists that Cross the Blood–Brain Barrier. *Neuropharmacology* **1999**, *38*, 1027–1034.
- (22) Richelson, E.; McCormick, D. J.; Pang, Y.-P.; Phillips, K. Peptide Analogs that are Potent and Selective for Human Neurotensin Receptor Subtype 2. U.S. Pat. Appl. Publ. WO 2008137720, 2009; *Chem. Abstr.* **2009**, *149*, 549259.
- (23) Bittermann, H.; Einsiedel, J.; Hübner, H.; Gmeiner, P. Evaluation of Lactam Bridged Neurotensin Analogues Adjusting  $\psi$ (Pro10) Close to the Experimentally Derived Bioactive Conformation of NT-(8–13). *J. Med. Chem.* **2004**, *47*, 5587–5590.
- (24) Haerterich, S.; Koschatzky, S.; Einsiedel, J.; Gmeiner, P. Novel Insights into GPCR–Peptide Interactions: Mutations in Extracellular Loop 1, Ligand Backbone Methylations and Molecular Modeling of Neurotensin Receptor 1. *Bioorg. Med. Chem.* **2008**, *16*, 9359–9368.
- (25) Einsiedel, J.; Hübner, H.; Hervet, M.; Härterich, S.; Koschatzky, S.; Gmeiner, P. Peptide Backbone Modifications on the C-Terminal Hexapeptide of Neurotensin. *Bioorg. Med. Chem. Lett.* **2008**, *18*, 2013–2018.
- (26) (a) Uno, T.; Beausoleil, E.; Goldsmith, R. A.; Levine, B. J.; Zuckermann, R. N. New Submonomers for Poly-N-Substituted Glycines (Peptoids). *Tetrahedron Lett.* **1999**, *40*, 1475–1478. (b) Shreder, K.; Zhang, L.; Gleeson, J.-P.; Ericsson, J. A.; Yalamoori, V. V.; Goodman, M. Solid Phase Organic Synthesis of Piperazineone Containing Enkephalin Mimetics: a Readily Derivatized, Traceless Scaffold. *J. Comb. Chem.* **1999**, *1*, 383–387.
- (27) Dechantsreiter, M.; Kessler, H.; Bernd, M.; Kutscher, B.; Beckers, T. Synthesis of Peptides with N-Substituted Glycines as Luteinizing Hormone-Releasing Hormone Inhibitory Analogs for Treatment of Hormone-Dependent Tumors. DE 19941248, 2000; *Chem. Abstr.* **2000**, *132*, 152142.
- (28) Ruijtenbeek, R.; Kruijtzter, J. A. W.; van de Wiel, W.; Fischer, M. J. E.; Flück, M.; Redegeld, F. A. M.; Liskamp, R. M. J.; Nijkamp, F. P. Peptoid–Peptide Hybrids that Bind Syk SH2 Domains Involved in Signal Transduction. *ChemBioChem* **2001**, *2*, 171–179.
- (29) Weber, D.; Berger, C.; Eickelmann, P.; Antel, J.; Kessler, H. Design of Selective Peptidomimetic Agonists for the Human Orphan Receptor BRS-3. *J. Med. Chem.* **2003**, *46*, 1918–1930.
- (30) Hemmi, K.; Neya, M.; Fukami, N.; Hashimoto, M.; Tanaka, H.; Kayakiri, N. Preparation of Peptides Having Endothelin Antagonist Activity and Pharmaceutical Compositions Comprising them. EP 457195 A2, 1991; *Chem. Abstr.* **1992**, *117*, 49261.
- (31) Henry, J. A.; Honvell, D. C.; Meecham, K. G.; Rees, D. C. A Structure–Affinity Study of the Amino Acid Side Chains in Neurotensin: N and C Terminal Deletions and Ala-Scan. *Bioorg. Med. Chem. Lett.* **1993**, *3*, 949–952.
- (32) Pang, Y.-P.; Cusack, B.; Groshan, K.; Richelson, E. Proposed Ligand Binding Site of the Transmembrane Receptor for Neurotensin-(8–13). *J. Biol. Chem.* **1996**, *271*, 15060–15068.
- (33) Gilbert, J. A.; McCormick, D. J.; Pfennig, M. A.; Kanba, K. S.; Enloe, L. J.; Moore, A.; Richelson, E. Neurotensin(8–13): Comparison of Novel Analogs for Stimulation of Cyclic GMP Formation in Neuroblastoma Clone N1E-115 and Receptor Binding to Human Brain and Intact N1E-115 Cells. *Biochem. Pharmacol.* **1989**, *38*, 3377–3382.
- (34) Mazella, J.; Vincent, J.-P. Functional Roles of the NTS2 and NTS3 Receptors. *Peptides* **2006**, *27*, 2469–2475.
- (35) Hill, S. J.; Baker, J. G.; Rees, S. Reporter-Gene Systems for the Study of G-Protein-Coupled Receptors. *Curr. Opin. Pharmacol.* **2001**, *1*, 526–532.
- (36) Els, S.; Beck-Sickinger, A. G.; Chollet, C. Ghrelin Receptors: High Constitutive Activity and Methods for Developing Inverse Agonists. *Method. Enzymol.* **2010**, *485*, 103–121.
- (37) Gully, D.; Labeuw, B.; Boigegrain, R.; Oury-Donat, F.; Bachy, A.; Poncelet, M.; Steinberg, R.; Franc, M.; Suaud-Chagny, O.; Santucci, V.; Vita, N.; Pecceu, F.; Labbé-Juillié, C.; Kitabgi, P.; Soubrié, P.; Le Fur, G.; Maffrand, J. P. Biochemical and Pharmacological Activities of SR 142948A, a New Potent Neurotensin Receptor Antagonist. *J. Pharm. Exp. Ther.* **1997**, *280*, 802–812.



(38) Richard, F.; Barroso, S.; Martinez, J.; Labbé-Jullié, C.; Kitabgi, P. Agonism, Inverse Agonism, and Neutral Antagonism at the Constitutively Active Human Neurotensin Receptor 2. *Mol. Pharmacol.* **2001**, *60*, 1392–1398.

(39) Holst, B.; Holliday, N. D.; Bach, A.; Elling, C. E.; Cox, H. M.; Schwartz, T. W. Common Structural Basis for Constitutive Activity of the Ghrelin Receptor Family. *J. Biol. Chem.* **2004**, *279*, 53806–53817.

(40) Orwig, K. S.; Lassetter, M. R.; Hadden, K.; Dix, T. A. Comparison of N-Terminal Modifications of Neurotensin(8–13) Analogues Correlates Peptide Stability but Not Binding Affinity with in Vivo Efficacy. *J. Med. Chem.* **2009**, *52*, 1803–1813.

(41) Bredeloux, P.; Cavalier, F.; Dubuc, I.; Vivet, B.; Costentin, J.; Martinez, J. Synthesis and Biological Effects of c(Lys-Lys-Pro-Tyr-Ile-Leu-Lys-Lys-Pro-Tyr-Ile-Leu) (JMV2012), a New Analogue of Neurotensin that Crosses the Blood–Brain Barrier. *J. Med. Chem.* **2008**, *51*, 1610–1616.

(42) Feifel, D.; Reza, T. L.; Wustrow, D. J.; Davis, M. D. Novel Antipsychotic-Like Effects on Prepulse Inhibition of Startle Produced by a Neurotensin Agonist. *J. Pharmacol. Exp. Ther.* **1999**, *288*, 710–713.

(43) Jordan, M.; Schallhorn, A.; Wurm, F. M. Transfecting Mammalian Cells: Optimization of Critical Parameters Affecting Calcium-phosphate Precipitate Formation. *Nucleic Acids Res.* **1996**, *24*, 596–601.

(44) Dörfler, M.; Tschammer, N.; Hamperl, K.; Hübner, H.; Gmeiner, P. Novel D3 Selective Dopaminergics Incorporating Enyne Units as Nonaromatic Catechol Bioisosteres: Synthesis, Bioactivity, and Mutagenesis Studies. *J. Med. Chem.* **2008**, *51*, 6829–6838.

(45) Hübner, H.; Haubmann, C.; Utz, W.; Gmeiner, P. Conjugated Enynes as Nonaromatic Catechol Bioisosteres: Synthesis, Binding Experiments and Computational Studies of Novel Dopamine Receptor Agonists Recognizing Preferentially the D3 Subtype. *J. Med. Chem.* **2000**, *43*, 756–762.

(46) Maschauer, S.; Einsiedel, J.; Haubner, R.; Hocke, C.; Ocker, M.; Hübner, H.; Kuwert, T.; Gmeiner, P.; Prante, O. Labeling and Glycosylation of Peptides Using Click Chemistry: A General Approach to 18F-Glycopeptides as Effective Imaging Probes for Positron Emission Tomography. *Angew. Chem., Int. Ed.* **2010**, *49*, 976–979.

(47) Lowry, O. H.; Rosebrough, N. J.; Farr, A. L.; Randall, R. J. Protein Measurement with the Folin Phenol Reagent. *J. Biol. Chem.* **1951**, *193*, 265–275.

(48) Cheng, Y.; Prusoff, W. H. Relationship between the inhibition constant ( $K_i$ ) and the concentration of inhibitor which causes 50 percent inhibition ( $IC_{50}$ ) of an enzymatic reaction. *Biochem. Pharmacol.* **1973**, *22*, 3099–3108.